DESIGN AND COMMISSIONING OF A MULTI-FREQUENCY DIGITAL LOW LEVEL RF CONTROL SYSTEM*

M. Konrad[†], U. Bonnes, C. Burandt, J. Conrad, R. Eichhorn,
J. Enders, P. Nonn, N. Pietralla, TU Darmstadt, Darmstadt, Germany

Abstract

Triggered by the need to control the superconducting cavities of the S-DALINAC, which have a high loaded quality factor and are thus very susceptible to microphonics, the development of a digital low level RF control system was started. The chosen design proved to be very flexible since other frequencies than the original 3 GHz may be adapted easily: The system converts the RF signal coming from the cavity (e. g. 3 GHz) down to the base band using a hardware I/Q demodulator. The base band signals are digitized by ADCs and fed into a FPGA where the control algorithm is implemented. The resulting signals are I/Q modulated before they are sent back to the cavity. The superconducting cavities are operated with a self-excited loop algorithm whereas a generator-driven algorithm is used for the low Q normal-conducting bunching cavities. A 6 GHz RF front end allows the synchronous operation of a new 2f buncher at the S-DALINAC. Meanwhile, a 325 MHz version has been built to control a pulsed prototype test stand for the p-LINAC at FAIR.

We will present the architecture of the RF control system as well as results obtained during operation.

INTRODUCTION

The S-DALINAC is an 130 MeV recirculating electron linac that is operated in cw mode. It uses superconducting niobium cavities at 2 K with a loaded Q of $3 \cdot 10^7$ for acceleration. Their 20 cell design and the high operating frequency of 3 GHz make them very susceptible for microphonics. In addition, superconducting 2 and 5 cell capture cavities, one of them providing a lower β, are used inside the injector.

Furthermore, room temperature chopper and buncher cavities are operated. A new polarized electron injector has been assembled in the accelerator hall recently [1]. Its bunching system consists of a chopper cavity and a 3 GHz as well as a 6 GHz harmonic buncher. This means that the RF control system has to deal with different Q_Ls from some 5000 to $3 \cdot 10^7$ as well as with different operating frequencies.

HARDWARE

The RF control system converts the RF signals down to the base band. This allows to split the hardware into two parts: A frequency dependent RF board containing the I/Q (de)modulator and a frequency independent FPGA board processing the signals. A separate power detector located on the RF board improves the accuracy of the magnitude measurement.

The current revision of the FPGA board evolved from several prototypes described in [2], [3], and [4]. It contains analog anti-aliasing filters with a cut-off frequency of 100 kHz to suppress the $19/20\,\pi$ mode of our cavities which is only 700 kHz away from the π mode used for acceleration. Compared to the hardware revision described in [4] an additional buffer stage has been inserted into the ADC path to keep the clock frequency of the high precision ADCs away from the fast ADCs. This eliminates an interference at 25 kHz that decisively degraded the performance.

The controllers for the 16 cavities are mounted into two 6 U crates. Both of them contain crate controller cards that couple the crates and allow a centralized digital readout. Two USB 2.0 interfaces allow streaming of diagnostic data to a server. This enables the operator to monitor all signals from inside the FPGA including all intermediary results of the signal processing. Over one of the interfaces 8 signals can be transmitted to the PC with the ADC's full sampling rate of 1 MS/s. The other interface will be used to transmit all signals with a lower sampling rate for monitoring.

At the S-DALINAC each superconducting cavity is equipped with two different tuners to control the eigenfrequency: A magnetostrictive tuner allows continuous fine tuning whereas a motor tuner provides a much wider tuning range. The power supplies for both tuners are connected to the FPGA boards via CAN bus.

CONTROL ALGORITHMS

For the normal-conducting resonators a Generator Driven Resonator (GDR) algorithm is used [4] whereas for the high Q superconducting cavities a Self-Excited Loop (SEL) algorithm is better suited.

In contrast to the GDR algorithm the SEL oscillates freely on a frequency that is determined by the eigenfrequency of the resonator and the loop phase. Thus this frequency can be locked to the frequency of a master oscillator by a controller that tunes the cavity's resonant frequency and/or applies an additional phase shift (phase-locked loop). The advantage of the SEL is that it immediately excites the cavity although the cavity's eigenfrequency might be detuned by many band widths. Furthermore the controller can recover from a breakdown even in

---

* Work supported by DFG through CRC 634 and by the BMBF under 06 DA 9024 I

[†] konrad@ikp.tu-darmstadt.de

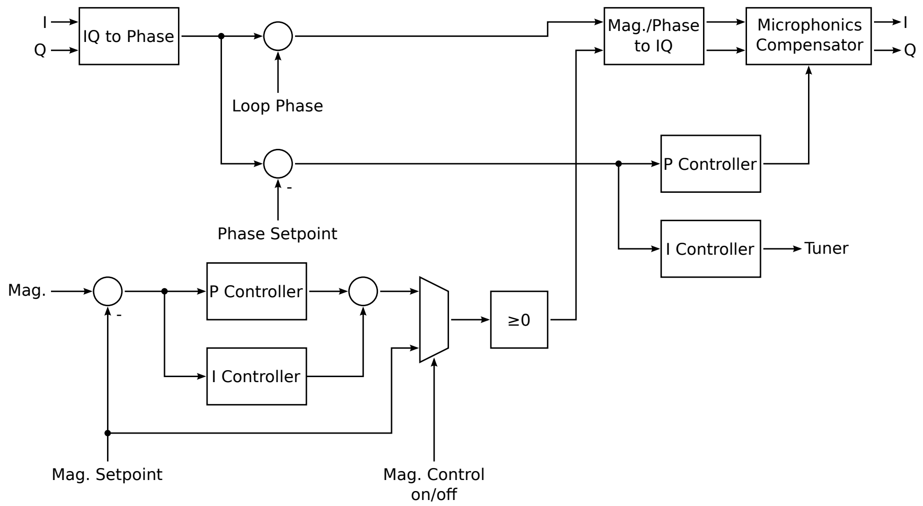

Figure 1: Block diagram of the SEL algorithm.

the presence of (static) Lorentz force detuning that might prevent a GDR from restarting oscillation.

Figure 1 shows a block diagram of the SEL algorithm. The I and Q signals are transformed into polar coordinates and back to Cartesian coordinates in the FPGA by the CORDIC algorithm [5]. Polar coordinates allow distinct controllers and parameters for magnitude and phase which is not possible if the controller operates in I/Q coordinates.

To avoid the excitation of mechanical eigenmodes the eigenfrequency of the resonator can only be tuned slowly. An integral controller is used for eigenfrequency control because it eliminates steady-state frequency offsets by tuning the SEL to exactly match the frequency of the master oscillator. Fast disturbances are compensated electrically. Instead of an actuator that simply shifts the phase a microphonics compensator [6] is used. This block adds an orthogonal correction vector to the input vector. If the length of this correction vector is proportional to the phase error the microphonics compensator has the inverse transfer function of the resonator. Thus phase and magnitude errors which always occur correlated if they are caused by detuning of the cavity are corrected in a single step. The microphonics compensator is used as an actuator for a proportional controller.

In addition to the microphonics compensator a magnitude controller is needed to compensate disturbances of the field amplitude. Again this is done by a proportional controller for fast disturbances which cannot completely be removed by the microphonics compensator whereas an integral controller removes the steady-state offset. The magnitude controller also compensates changes of the accelerating field strength caused by beam current fluctuations.

The motor tuner is equipped with a three-step switching controller that automatically activates the motor if the fine tuner approaches its limits. The motor tuner causes vibrations and that way increases the amount of microphonics the RF control system has to deal with. That is why the hysteresis of the three-step controller has been defined so that the cavity is always tuned to the middle of the fine tuner's controlling range once the motor has been activated. This behavior makes sure the motor is only seldom activated. The motor tuner is inhibited if the RF signal is switched off by the operator or the RF interlock to avoid that small offsets or noise lead to a detuning of the cavity.

COMMISSIONING AND MEASUREMENTS

The performance of the SEL algorithm has been measured operating a 20 cell cavity in the cryo-module of the S-DALINAC at a typical field strength of 4 to 5 MeV. Figure 2(a) shows the integrated phase error during SEL operation while all controllers are switched off. The plot was created by means of a Fourier transformation of the residual error and integration of the RMS error from zero up to the frequency given on the abscissa. The total magnitude of the phase fluctuations is $2.4\,^\circ$ rms. By turning on the phase controller these fluctuations can be reduced to a value below $0.3\,^\circ$ rms [4]. If both phase and magnitude controllers are activated it becomes more difficult to reduce phase as well as magnitude fluctuations. A trade-off between phase and magnitude errors has to be made. In Fig. 2(b) the parameters of the controllers have been chosen to damp the phase fluctuations to a value of roughly $0.7\,^\circ$ rms which is our target specification. Figure 3(b) shows the corresponding magnitude error that has been recorded at the same time. Compared to Fig. 3(a) the magnitude controller reduces the magnitude fluctuations significantly to $\Delta M/M = 7.2 \cdot 10^{-5}$ rms being also marginally below specification.

The source of the noticeable high amplitudes at frequencies above 10 kHz is not yet known. They only appear if the phase controller is active (with the same parameters that were optimized for small residual errors with both controllers enabled) while the magnitude controller is switched

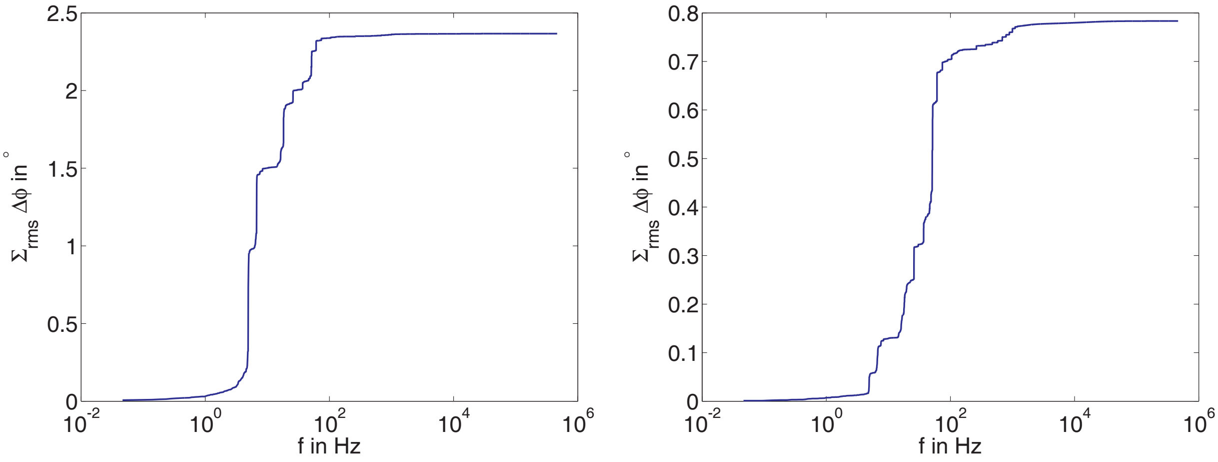

(a) Magnitude and phase controller deactivated.

(b) Magnitude and phase controller activated.

Figure 2: Integrated amplitude spectra of phase error of the SEL.

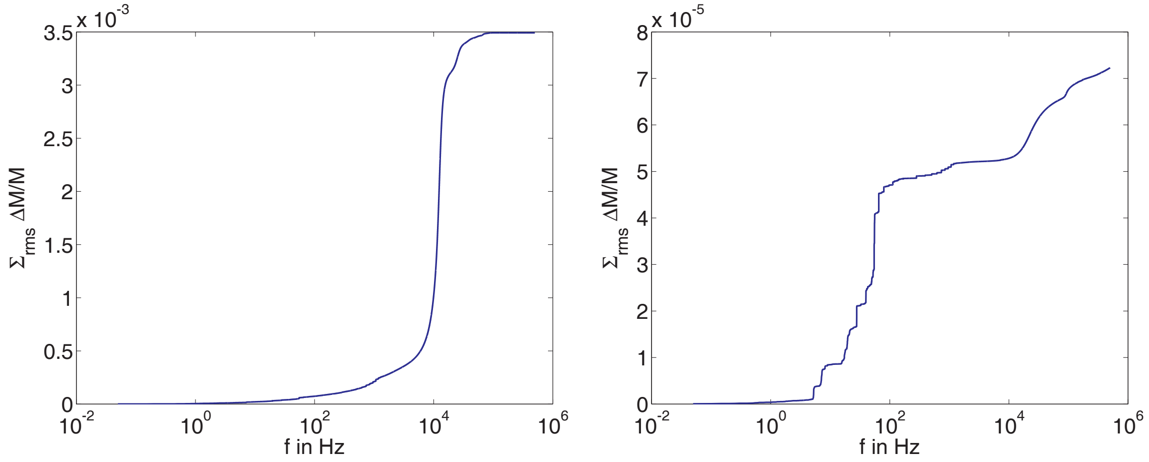

(a) Phase controller activated, magnitude controller deactivated.

(b) Magnitude and phase controller activated.

Figure 3: Integrated amplitude spectra of relative magnitude error of the SEL.

off.

During commissioning it turned out that the RF control system is sensitive enough to roughly detect the phase of the field induced in a switched off cavity by an electron beam of about 1 μA (pick-up operation). This allows the operator to quickly determine the right phase relationship between consecutive cavities when the distance between cavities has changed e. g. due to maintenance of a cryomodule.

SUMMARY

The new RF control system has completely replaced the old analog system. In up to date some 1000 hours of beam time it has proven to be much more reliable than the old one. Improved FPGA boards as well as enhanced control algorithms using integral as well as proportional controllers reduce the residual errors in magnitude and phase significantly to $\Delta M/M = 7.2 \cdot 10^{-5}$ rms and $\Delta\phi = 0.78°$ rms.

REFERENCES

[1] C. Eckardt et al., “The S-DALINAC Polarized Injector SPIN – Performance and Results”, Proceedings of PAC 2011, New York, USA.

[2] A. Araz et al., “Development of a new Low-Level RF-Control-System for the S-DALINAC”, Proceedings of EPAC 2008, Genoa, Italy, p. 1391.

[3] A. Araz et al., “The Baseband Low Level RF Control for the S-DALINAC: A flexible Solution for other Frequencies?”, Proceedings of SRF 2009, Berlin, Germany, p. 689.

[4] M. Konrad et al., “A Digital Low Level RF Control System for the S-DALINAC”, Proceedings of LINAC 2010, Tsukuba, Japan, p. 268.

[5] J. Volder, “The CORDIC Trigonometric Computing Technique”, IRE Transactions on Electronic Computers, pp. 330-334, September 1959.

[6] J. Delayen, “Phase and Amplitude Stabilization of Superconducting Resonators”, Ph. D. Thesis, California Institute of Technology, 1978.